Atomic Spectroscopy

Article

Ultra-Trace Detection of Methyl Parathion in Traditional Chinese Medicines by Gold Filament Enrichment Point Discharge Chemical Vapor Generation Atomic Emission Spectrometry

Xin Yuan,[a,*] Yanping Wang,[a] Yuanjiao Yang,[a] Mei Zhang,[a] and Ke Huang [b,*]

[a] State Key Laboratory of Southwestern Chinese Medicine Resources, School of Pharmacy, Chengdu University of Traditional Chinese Medicine, Chengdu 611137, P. R. China

[b] College of Chemistry and Material Science, Sichuan Normal University, Chengdu 610068, P. R. China

Received: *August 26, 2024;* ***Revised:*** *September 25, 2024;* ***Accepted:*** *September 26, 2024;* ***Available online:*** *September 26, 2024.*

DOI: 10.46770/AS.2024.198

ABSTRACT: The increasing global popularity of traditional Chinese medicines (TCMs) raises significant concerns about potential contamination with organophosphorus pesticides (OPs). Portable analytical methods are particularly valuable for on-site pesticide analysis, enabling rapid screening and enhancing the safety assurance of TCM products. This study investigates the use of miniaturized microplasma atomic emission spectrometry (AES) as a promising tool for methyl parathion (MP) analysis in TCMs, leveraging the inhibition effect of OPs on butyrylcholinesterase (BChE) within a gold filament enrichment coupling point discharge chemical vapor generation atomic emission spectrometry (PD-CVG-AES) system. Specifically, BChE catalyzes the hydrolysis of acetylthiocholine chloride (ATCh) to form thiocholine (TCh), which contains sulfhydryl groups (-SH) that can strongly bind with Hg^{2+}, leading to less efficient vapor generation and reduced AES signals of Hg^{2+}. However, OPs like MP inhibit BChE activity and suppress TCh generation, resulting in the recovery AES signals. Ultra-trace levels of MP can be indirectly detected due to the high sensitivity of Hg^{2+} analysis using the gold filament enrichment PD-AES system. Under optimal conditions, the limit of detection (LOD) for the MP assay was 13 ng mL^{-1} within a range of 0.5 to 10 μg mL^{-1}, with a relative standard deviation (RSD, n=5) of 0.8%. This analytical approach has proven effective in the detection of MP in TCMs, with advantages including ease of use and affordability.

INTRODUCTION

Organophosphorus pesticides (OPs) are widely used in agriculture and forestry to prevent and control various threats, such as diseases, insects, weeds, and other pests.[1] However, excessive application of OPs can result in food contamination and environmental pollution.[2,3] Once absorbed by the human body, OPs inhibit cholinesterase activity, potentially causing neurotoxicity and even death.[4,5] The use of pesticides, including OPs, is common in the production of traditional Chinese medicines (TCMs). Methyl parathion (MP), chlorpyrifos, and other highly toxic, banned OPs have been repeatedly detected in TCMs, hindering the industry's development. Consequently, developing a sensitive and straightforward method for the rapid analysis of MP is of great importance for public and environmental safety.

Chromatography,[6,7] mass spectrometry,[8,9] immunoassays,[10,11] and enzyme inhibition methods[12,13] are widely used for OPs detection. The Chinese Pharmacopoeia (2020 edition) outlines

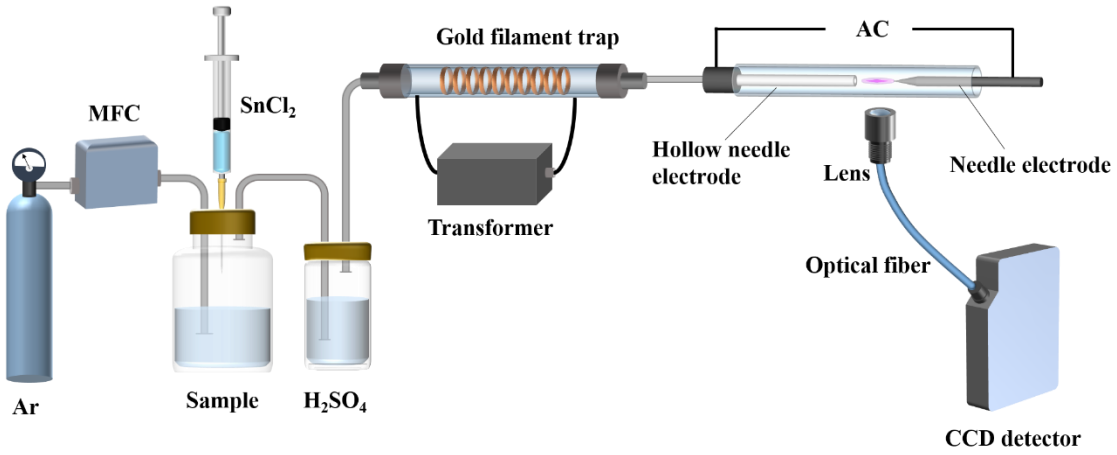

Fig. 1 Schematic diagram of PD-CVG-AES system. AC, alternating current; and MFC, mass flow controller.

chromatography and gas chromatography-tandem mass spectrometry (GC-MS) as the designated methods for OP determination. These techniques are recognized for their well-established technology, high sensitivity, and robust anti-interference properties.[14] However, these methods rely on expensive, large-scale instrumentation, specialized laboratories, and highly trained technicians. Immunoassays rely on the specific binding of antigens and antibodies to detect target pesticides. However, the preparation of these antigens and antibodies is complex, costly, and requires strict environmental conditions.[15] The enzyme inhibition method relies on the principle that OPs effectively inhibit cholinesterase activity. OPs are indirectly analyzed through the relationship between enzyme inhibition ratesand pesticide concentration.[16,17] Cholinesterase, commonly used in enzyme inhibition assays, universally responds to OPs, is readily available, and is cost-effective.[18] Recently, many colorimetric and fluorescent studies have integrated enzyme inhibition methods with nanomaterials to enhance OP detection sensitivity significantly.[19,20] However, the preparation of nanomaterials is often labor-intensive and time-consuming.

Atomic spectrometry (AS) offers excellent resistance and high sensitivity, making it one of the most efficient methods for elemental analysis.[21,22] In recent years, continuous innovations in AS technology have expanded its range of detection targets, and AS has been successfully applied in bio-analysis and small molecule analysis.[23-27] However, commercial AS instruments still face challenges such as high cost, high energy consumption, and limited applicability for point-of-care testing (POCT). Microplasmas, encompassing techniques like corona discharge (CD), dielectric barrier discharge (DBD), glow discharge (GD), cathode glow discharge (CGD), and point discharge (PD), are notable for their compact size, low energy requirements, affordability, and potential for real-time field analysis.[28-32] AS has been successfully miniaturized by employing microplasmas as ionization sources, which have been effectively utilized in indirect bio-analysis.[29,33] For example, Yang *et al.* employed PD-AES for the indirect determination of oxalate in clinical urolithiasis samples.[34] In our previous work, we successfully integrated microplasma technology with AES to detect ascorbic acid in TCM samples.[35]

This study presents a novel, sensitive analytical method for MP detection. The platform combines gold filament enrichment with a PD-CVG-AES system, which is highly sensitive for Hg^{2+} detection. The method exploits the inhibitory effect of OPs on butyrylcholinesterase (BChE) activity to establish a quantitative relationship between MP and Hg^{2+} concentration. Consequently, MP analysis was indirectly achieved through the measurement of the AES Hg signal. The proposed method has been successfully applied for the accurate determination of MP in four TCMs and artificially cultivated fresh Mentha samples, yielding satisfactory results.

EXPERIMENTAL

Instrumentation and reagents. The PD-CVG-AES system was constructed similarly to our previous work.[35] Fig 1 presents a schematic diagram of the PD-CVG-AES system. The system comprises a carrier gas system, an AC power supply, a cold vapor generation system, a gold filament enrichment tube, a point discharge microplasma source, and a spectrometer. A detailed description of the instrument's construction and operation procedures can be found in the Supporting Information (SI). Table S1 outlines the operational parameters of the PD-CVG-AES, and the reagents used are also detailed in the SI.

Analytical procedure. A 100 μL solution containing varying concentrations of MP and 100 μL of BChE (1000 U/L) was mixed with 200 μL of PBS (10 mM, pH 7.4) and incubated for 30 min.

Subsequently, 100 µL of ATCh (2.5 mM) was added and incubated for an additional 20 min. The mixture was then treated with 200 µL of Hg^{2+} solution (80 ng/mL), allowed to react at room temperature for 1 min, and finally diluted to 10 mL with ultrapure water.

Sample preparation. The QuEChERS method was used to extract MP from TCMs (Panax ginseng, radix paeoniae alba, angelica sinensis, and Lonicera japonica).[36,37] 3 g of the sample powder, sieved through a No. 3 sieve (Aperture 355 ±13 µm), was accurately weighed into a 50 mL centrifuge tube. To the tube, 15 mL of 1% (v/v, %) glacial acetic acid was added, and thorough mixing was ensured by vortexing, after which the mixture was allowed to stand for 30 min. Acetonitrile (15 mL) and 7.5 g of a mixture of anhydrous magnesium sulfate and anhydrous sodium acetate in a 4:1 ratio was then added to the tube. The tube containing the mixture was cooled in an ice bath for 10 min, followed by centrifugation at 4000 rpm for 5 min. 9 mL of the supernatant was transferred to a dispersed solid-phase extraction clean-up tube, shaken vigorously for 5 minutes, and centrifuged again at 4000 rpm for 5 minutes. 5 mL of the supernatant was transferred to a nitrogen blower, and the solution was concentrated to approximately 0.4 mL. The concentrate was diluted to 1 mL with acetonitrile, and the final solution was subsequently filtered through a 0.22 µm nylon injection filter.

The extraction of MP from fresh Mentha samples was conducted using the QuEChERS pre-treatment method, as outlined in "Determination of 208 Pesticide and Metabolite Residues in Foods of Plant Origin".[38,39] Six pots of fresh Mentha were purchased from the market and cultivated for two weeks. Afterward, they were divided into two groups and sprayed with MP at concentrations of 0.4 mg mL^{-1} and 0.8 mg mL^{-1} once a week for four consecutive weeks. Later, fresh Mentha was harvested, and 10 g of Mentha samples were accurately weighed and ground into a homogeneous paste using a tissue masher. The sample was transferred to a centrifuge tube. To the tube, 10 mL of acetonitrile, 4 g of magnesium sulfate, 1 g of sodium chloride, 1 g of sodium citrate, 0.5 g of disodium hydrogen citrate, and a ceramic homogenizer were added. The mixture was vortexed vigorously for 1 minute and centrifuged at 4200 rpm for 5 minutes. The supernatant was transferred to a clean centrifuge tube. To the supernatant, 900 mg of magnesium sulfate and 150 mg of PSA (N-(N-propyl)ethylenediamine) were added. The mixture was vortexed for 1 min and centrifuged at 4200 rpm for 5 min. The supernatant was filtered through a 0.22 µm nylon filter membrane.

RESULTS AND DISCUSSION

Feasibility of the PD-CVG-AES system for Hg^{2+} detection. In the PD-CVG-AES system, Hg^{2+} was reduced by $SnCl_2$ to Hg^0 vapor, which was carried by the carrier gas (argon) to the gold filament enrichment tube, where it reacted with gold to form gold amalgam. Subsequently, by heating the electric stove wire outside the tube, the Hg^0 vapor adsorbed on the gold filament was desorbed and entered the PD microplasma source to be excited. Finally, the AES signal of Hg^{2+} at 253.67 nm was collected by a portable CCD (charge coupled device) spectrometer. As shown in Fig. S1, the solution of 20 ng mL^{-1} Hg^{2+} (Fig. S1A) exhibited a clear AES signal at 253.67 nm, whereas the blank (Fig. S1B) did not. This observation indicates that the PD-CVG-AES system is feasible for the analysis of Hg^{2+}. To verify whether gold filament enrichment provides a signal amplification effect, the signal response of the same concentration of Hg^{2+} solution (20 ng mL^{-1}) with and without gold filament enrichment was compared. As shown in Fig. S2, the signal was amplified by approximately 16.28 times when using gold filament enrichment (Fig. S2A), and the detection time was significantly shorter than in the blank group (Fig. S2B). Therefore, the use of gold filament preconcentration is not only feasible but also beneficial, as it shortens detection time and amplifies the signal.

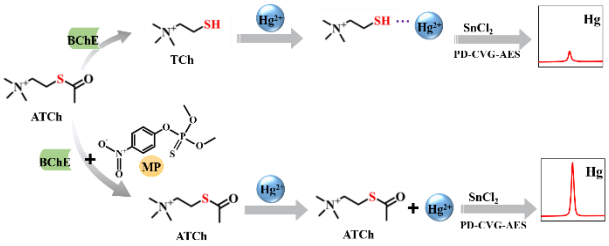

Scheme 1. Schematic illustration for MP detection based on PD-CVG-AES system.

Feasibility of MP detection by PD-CVG-AES. The determination of MP in this work is primarily based on the principle of enzyme inhibition. BChE effectively catalyzes the hydrolysis of ATCh to TCh, which contains -SH groups. These -SH groups can form a strong chemical bond with Hg^{2+}, thereby hindering the CVG process of Hg^{2+} and resulting in a decreased AES signal.[40] It is well known that OPs inhibit BChE activity, thereby preventing the hydrolysis of ATCh and subsequently restoring the AES signal of Hg^{2+}. Using this strategy, the indirect analysis of MP can be achieved by determining Hg^{2+} with the PD-CVG-AES system. The schematic diagram of this process is shown in Scheme 1.

To verify the feasibility of this method, the intensity of the AES signal was compared across different concentrations of enzymes and pesticides. As shown in Fig. 2a and 2b, the AES signals of Hg^{2+} remained almost unchanged after the addition of 5 mM ATCh, indicating that the CVG process of Hg^{2+} was not influenced by ATCh. However, as the concentration of BChE increased, the signal gradually weakened (Fig. 2c and 2d). After the addition of

MP, the AES signal of Hg^{2+} recovered, with a stronger signal observed at higher MP concentrations (Fig. 2e and 2f). These results demonstrate that BChE can inhibit the AES signal of Hg^{2+}, while MP restores it, confirming the feasibility of this method.

Optimization of PD. The discharge stability of the PD microplasma source is closely related to the discharge voltage and the discharge distance. The discharge voltage was optimized within the range of 500 V to 1750 V. As shown in Fig. S3A, the AES signal of Hg^{2+} gradually increased and then decreased as the applied voltage was raised. This phenomenon can be attributed to the fact that a low discharge voltage lacked sufficient excitation capacity for Hg^0 vapor, while an excessively high voltage led to discharge instability. Consequently, 1250 V was determined to be the optimal discharge voltage. The electrode distance affects not only the physical properties of the microplasma but also the diffusion, interaction, and excitation processes of the analyte. The effect of discharge distance, ranging from 0.5 to 4 mm, was investigated. As illustrated in Fig. S3B, the AES signal peaked when the distance between the two electrodes was 1 mm. The signal gradually decreased as the distance between the electrodes increased, likely due to the unstable discharge caused by the excessive distance. Therefore, 1 mm was selected as the optimal discharge distance.

Optimization of pre-enrichment parameters. The argon flow rate during the pre-enrichment process is primarily associated with the enrichment efficiency of Hg^0 vapor on the gold filament. If the argon flow rate is too high, the Hg^0 vapor generated by CVG will pass through the gold filament enrichment tube too quickly, preventing complete reaction with the gold and thereby reducing enrichment efficiency. Conversely, a flow rate that is too low will extend the enrichment time. In this experiment, an argon flow rate ranging from 100 to 500 mL min^{-1} was investigated. As shown in Fig. S3C, a peak in the AES signal was observed at a flow rate of 150 mL min^{-1}. At this flow rate, the Hg^0 vapor generated in the sample vial could be fully purged by argon within 8 min (Fig. S3D). Therefore, an argon flow rate of 150 mL min^{-1} with an 8-minute purge was selected as the optimal condition for the pre-enrichment process.

Optimization of the argon flow rate in the thermal desorption step. In the thermal desorption process, argon functions not only as a carrier gas but also as a working gas for the PD microplasma source. The argon flow rate significantly affects both the thermal desorption efficiency and the energy stability of the plasma. Flow rates of argon ranging from 100 to 500 mL min^{-1} were examined. The highest AES signal for Hg^{2+} was achieved at an argon flow rate of 300 mL min^{-1} (Fig. S3E). At lower argon flow rates, the Hg^0 vapor generated by thermal desorption disrupted the stability of the microplasma, resulting in discharge instability and a decrease in signal intensity. Conversely, when the argon flow rate exceeded 300 mL min^{-1}, the AES signal gradually diminished as the argon flow rate continued to rise. This decrease was attributed to the dilution of Hg^0 vapor concentration due to the higher argon flow rate. Therefore, an argon flow rate of 300 mL min^{-1} was selected as the optimal flow rate for the thermal desorption process.

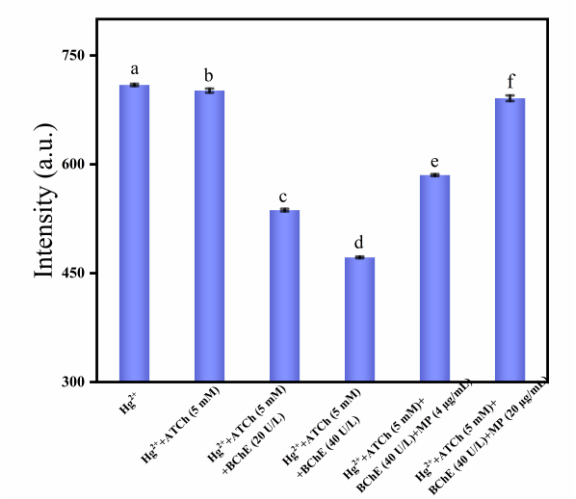

Fig. 2 Feasibility study of PD-CVG-AES system to detect MP. Error bars originated from triplicate measurements.

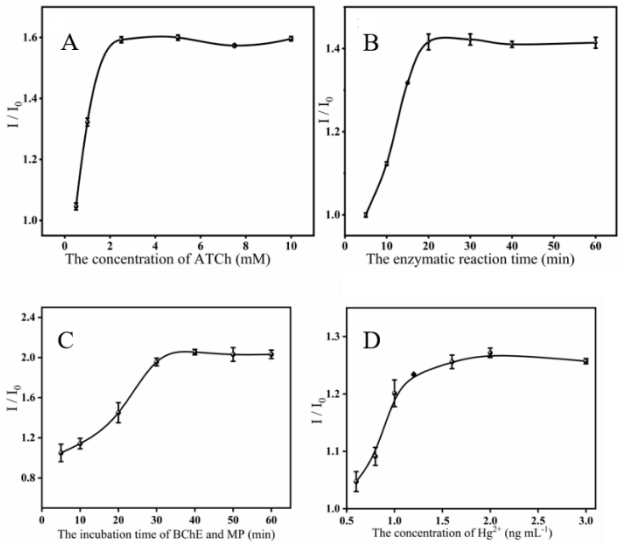

Fig. 3 Optimization of enzymatic reaction conditions. (A) Optimization of the concentration of ATCh (mM); (B) Optimization of the enzymatic reaction time (min). (C) Optimization of the incubation time of BChE and MP (min), (D) Effect of the concentration of Hg^{2+}. Error bars originated from triplicate measurements.

Optimization of enzymatic reaction conditions. Several experimental conditions influence the rate and completeness of the hydrolysis reaction between BChE and ATCh, including enzymatic reaction time, ATCh concentration, incubation temperature, and solution pH. BChE, a hydrolase commonly found in the peripheral systems of animals, has been shown in

numerous studies to have optimal catalytic conditions at 37°C and pH 7.4. Therefore, the concentrations of ATCh and enzymatic reaction time were optimized at a temperature of 37°C and a pH of 7.4.

ATCh concentrations significantly impact the rate of the enzymatic reaction. As ATCh concentration increases, BChE becomes gradually saturated, and the reaction rate approaches its maximum. The optimal concentration of ATCh was investigated within the range of 0.5 to 10 mM. As illustrated in Fig. 3A, the ratio I/I_0 (where I/I_0 represents the ratio of the AES signal of Hg^{2+} with and without MP added to the sample solution) initially increased. After the ATCh concentration reached 2.5 mM, the curve stabilized, indicating that BChE and ATCh had largely reacted completely. Consequently, an ATCh concentration of 2.5 mM was selected for subsequent experiments.

In optimizing enzymatic reaction time, we assessed the effects of reaction durations ranging from 5 to 30 min. As illustrated in Fig. 3B, the I/I_0 ratio peaked at a reaction time of 20 minutes and remained stable thereafter. This indicates that ATCh had completely reacted with BChE after 20 min of incubation. Therefore, a reaction time of 20 min was determined to be optimal for the enzymatic reaction.

Optimization of the incubation time of BChE and MP. To achieve optimal analytical performance for detecting MP using this method, it is essential to allow sufficient incubation time for the enzyme activity to be effectively inhibited by MP. The ratio of I/I_0 was evaluated over a range of incubation times, from 5 to 60 minutes. The results are depicted in Fig. 3C. As illustrated, the I/I_0 ratio peaked and stabilized at 30 min, indicating that butyrylcholinesterase (BChE) in the solution was effectively inhibited by MP. Consequently, an incubation time of 30 min was selected as the optimal experimental condition.

Hg^{2+} poses significant risks to both human health and the environment. To improve analytical performance while minimizing the use of Hg^{2+} solution, the concentration of Hg^{2+} was optimized within the range of 0.6 to 3 ng mL^{-1}. As shown in Fig. 3D, the curve stabilized and became smooth at a concentration of 1.6 ng mL^{-1}. Therefore, to ensure a stable signal and reduce the use of Hg^{2+}, the concentration of 1.6 ng mL^{-1} was selected for the experiment.

Interference study. Due to the complexity of TCM sample compositions, interference may arise during the actual detection process. To assess method selectivity, a variety of potential interfering substances were examined after QuEChERS procedure. The selectivity of the proposed method was evaluated by examining various ions and small molecules, including Na^+, Fe^{2+}, Fe^{3+}, Cu^{2+}, Zn^{2+}, ascorbic acid (AA), Ethylene Diamine Tetraacetic Acid (EDTA), Sucrose, L-Histidine (L-His), Aspartic Acid (Asp), and Tyrosine (Tyr), which are components commonly found in buffers used in QuEChERS or widely present in TCM samples. As presented in Table 1, no significant interference with the analysis was observed even with coexisting substances up to 100 times higher than the concentration of MP. The recovery rate of MP ranged between 98% and 109%. These results indicate that this method has high selectivity for MP and establishes a basis for the analysis of TCM samples. Moreover, various pesticides were selected to assess the interference effects of MP using the proposed method. As shown in Fig. S4, both OPs and carbamate pesticides were able to restore the signal of atomic emission spectrometry for mercury ions, while neonicotinoid insecticides did not have this effect. This is attributed to the fact that both OPs and CPs inhibit the activity of BChE.[41, 42]

Table 1. Interference of coexisting substance

Interference	[Interference] μg mL^{-1}	[MP] μg mL^{-1}	Recovery (%)
Na^+	100	1	99
Fe^{2+}	100	1	102
Fe^{3+}	100	1	101
Zn^{2+}	100	1	103
Cu^{2+}	100	1	106
AA	100	1	109
EDTA	100	1	100
Sucrose	100	1	99
L-His	100	1	102
Tyr	100	1	106
Asp	100	1	98

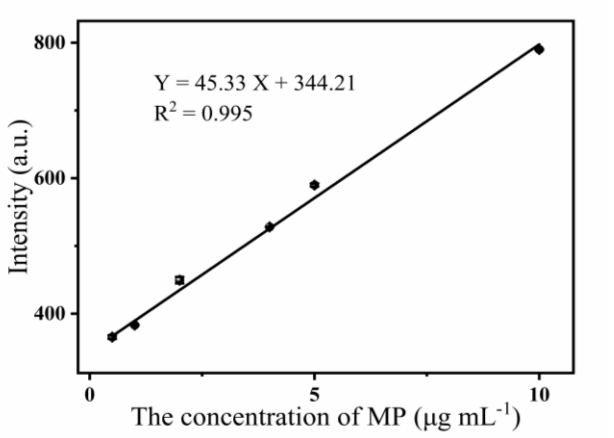

Fig. 4 Analytical performance of MP by PD-CVG-AES. Calibration curve at concentrations of MP ranging from 0.5 ~ 10 μg mL^{-1}. Experimental conditions: the concentration of Hg^{2+}, 1.6 ng mL^{-1}; the concentration of ATCh: 2.5 mM; the concentration of BChE: 10 U/L; the enzymatic reaction time: 20 min; the reaction time of BChE and MP: 30 min. Error bars originated from triplicate measurements.

Analytical figures of merit. Under optimized experimental conditions, the analytical performance for detecting MP was evaluated. As shown in Fig. 4, within the MP concentration range of 0.5 to 10 μg mL^{-1}, the AES signal of Hg^{2+} gradually increased and exhibited a strong linear relationship with MP concentration. The linear equation was Y = 45.33X + 344.21, and the linear

Table 2. Analytical results of MP contents in TCM samples

Sample	Added/ng g^{-1}	Found/ng g^{-1}	Recovery (%)
Panax ginseng	0	-	-
	4.5	4.75 ± 0.73	105
Radix paeoniae alba	0	-	-
	4.5	4.70 ± 0.70	105
Angelica sinensis	0	-	-
	4.5	5.00 ± 0.56	111
Lonicera japonica	0	-	-
	4.5	4.65 ± 0.98	103
Mentha canadensis Linnaeus 1	0	27.95 ± 0.23	-
	4.5	32.45 ± 0.13	100
Mentha canadensis Linnaeus 2	0	8.75 ± 0.37	-
	4.5	13.6 ± 0.04	108

correlation coefficient (R) was 0.997. The limit of detection (LOD = 3σ/S, where σ and S are the relative standard deviation of 11 blank samples and the slope of the calibration curve, respectively) was calculated to be 13 ng mL^{-1}, with a relative standard deviation (RSD, n = 5) of 0.8% when the MP concentration was 1 μg mL^{-1}. In comparison with other available studies, including spectroscopy, chromatography, electrochemistry, GC-MS, and other methods, the detection limit of this approach was found to be comparable or even lower (as shown in Table S2). Additionally, it offers the advantages of ease of use and affordability, making it a competitive and practical alternative for detecting MP.

Real TCMs samples analysis. To further verify the accuracy of the PD-CVG-AES analysis system for detecting MP in TCMs, Panax ginseng, Radix Paeoniae Alba, Angelica sinensis, Lonicera japonica, and artificially cultivated *Mentha* samples were analyzed. MP was not detected in the four dried herbs, while the MP content in artificially cultivated Mentha samples was recorded at 27.95 ng g^{-1} and 8.75 ng g^{-1}, respectively. According to the Chinese Pharmacopoeia, the MP content in traditional Chinese medicines (TCMs) should not exceed 0.02 mg kg^{-1}. All tested samples complied with this regulation, except for the artificially sprayed Mentha sample, which contained 0.8 mg mL^{-1}. To evaluate the practicability of the method, a 4.5 ng g^{-1} MP standard solution was added to the sample. The analytical results are summarized in Table 2, which indicates that the recovery ranged from 100% to 111%, thereby confirming its suitability for the analysis of real samples.

CONCLUSION

The PD-CVG-AES system was successfully used for analysis of MP in TCM samples. It exhibited excellent linearity in the MP concentration range of 0.5 to 10 μg mL^{-1}, achieving a LOD of 13 ng mL^{-1}. This method demonstrated promising performance for MP determination in TCM samples. In comparison to larger-scale techniques like GC and HPLC, the miniaturized microplasma AES system offers significant advantages, including high sensitivity, operational simplicity, low energy consumption, compact size, and cost-effectiveness. However, since both OPs and chlorpyrifos (CPs) inhibit BChE activity, this method lacks specificity for these pesticides. Therefore, specific assays for different pesticides need to be developed in the future to improve detection specificity. One promising approach to enhance the method's selectivity is through the use of aptamers. Incorporating aptamer technology could improve the ability to specifically recognize certain pesticides, thereby increasing the assay's specificity. Additionally, integrating nanomaterials or biosensor technologies could further enhance the selectivity and sensitivity of the detection method, ensuring accurate detection of different pesticides.

ASSOCIATED CONTENT

Supporting information (Figs. S1-S4 and Table S1-S2) is available at www.at-spectrosc.com/as/home

AUTHOR INFORMATION

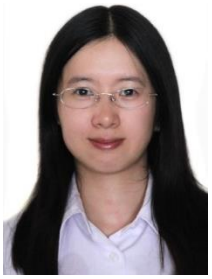

Xin Yuan is an associate professor at the Chengdu University of Traditional Chinese Medicine. She received her BSc degree in 2010 from the College of Chemistry and Chemical Engineering, Southwest University, Ph.D. degree in 2015 in analytical chemistry from Sichuan University. She began her own independent career in the College of Pharmacy, Chengdu University of Traditional Chinese Medicine. Her current research interests are analytical instruments and their pesticide analysis application. Xin Yuan is the author or co-author of over 40 articles published in peer-reviewed scientific journals.

Ke Huang is a professor at the Sichuan Normal University. He received his BSc degree in 2010 from the College of Chemistry, Sichuan University, Ph.D. degree in 2015 in analytical chemistry from the College of Chemistry, Sichuan University. He began his independent career in the College of Chemistry and Material Science, Sichuan Normal University. His current research interest is atomic spectroscopy bioanalysis. He has been working as member of editorial board for *Atomic Spectroscopy*. Ke Huang is the author or co-author of over 100 articles published in peer-reviewed scientific journals.

Corresponding Author

* X. Yuan

Email address: yuanxin0330@163.com

* Ke Huang

Email address: huangke@sicnu.edu.cn

Notes

The authors declare no competing financial interest.

ACKNOWLEDGMENTS

The authors thank the National Natural Science Foundation of China (21605108 & 82474074), Sichuan Science and Technology Program (2023NSFSC1090), and Foundation of Sichuan Normal University (ZZYQ2022002 & SYJS2022011) for financial support.

REFERENCES

1. J. Kaushal, M. Khatri, and S. K. Arya, *Ecotoxicol. Environ. Saf.*, 2021, **207**, 111483. https://doi.org/10.1016/j.ecoenv.2020.111483
2. K. H. Kim, E. Kabir, and S. A. Jahan, *Sci. Total Environ.*, 2017, **575**, 525-535. https://doi.org/10.1016/j.scitotenv.2016.09.009
3. P. Nicolopoulou-Stamati, S. Maipas, C. Kotampasi, P. Stamatis, and L. Hens, *Front. Public Health*, 2016, **4**, 148. https://doi.org/10.3389/fpubh.2016.00148
4. M. B. Colovic, D. Z. Krstic, T. D. Lazarevic-Pasti, A. M. Bondzic, and V. M. Vasic, *Curr. Neuropharmacol.*, 2013, **11**, 315-335. https://doi.org/10.2174/1570159x11311030006
5. V. A. Rauh, F. P. Perera, M. K. Horton, R. M. Whyatt, R. Bansal, X. J. Hao, J. Liu, D. B. Barr, T. A. Slotkin, and B. S. Peterson, *Proc. Natl. Acad. Sci. U.S.A.*, 2012, **109**, 7871-7876. https://doi.org/10.1073/pnas.1203396109
6. R. Loos, R. Carvalho, D. C. António, S. Cornero, G. Locoro, S. Tavazzi, B. Paracchini, M. Ghiani, T. Lettieri, L. Blaha, B. Jarosova, S. Voorspoels, K. Servaes, P. Haglund, J. Fick, R. H. Lindberg, D. Schwesig, and B. M. Gawlik, *Water Res.*, 2013, **47**, 6475-6487. https://doi.org/10.1016/j.watres.2013.08.024
7. Y. C. Pan, X. Liu, J. Liu, J. P. Wang, J. X. Liu, Y. X. Gao, and N. Ma, *Food Chem. X*, 2022, **15**, 100424. https://doi.org/10.1016/j.fochx.2022.100424
8. A. Y. Liu, W. Kou, H. Zhang, J. Q. Xu, L. X. Zhu, S. L. Kuang, K. Huang, H. W. Chen, Q. Jia, *Anal. Chem.*, 2020, **92**, 4137-4145. https://doi.org/10.1021/acs.analchem.0c00304
9. Z. H. Ma, Y. J. Gao, F. J. Chu, Y. L. Tong, Y. W. He, Y. Li, Z. Gao, W. W. Chen, S. H. Zhang, Y. J. Pan, *Chin. Chem. Lett.*, 2022, **33**, 4411-4414. https://doi.org/10.1016/j.cclet.2021.12.029
10. K.-O. Kim, Y. J. Kim, Y. T. Lee, B. D. Hammock, and H.-S. Lee, *Anal. Chem.*, 2002, **50**, 6675-6682. https://doi.org/10.1021/jf025703
11. J. J. Yao, Z. X. Wang, L. L. Guo, X. X. Xu, L. Q. Liu, L. G. Xu, S. S. Song; C. L. Xu, and H. Kuang, *TRAC-Trend. Anal. Chem.*, 2020, **131**, 116022. https://doi.org/10.1016/j.trac.2020.116022
12. X. J. Dong, Z. Y. Tang, H. Zhang, Y. Hu, Z. Y. Yao, R. Y. Huang, J. Bai, Y. Yang, W. J. Hong, *Anal. Chem.*, 2023, **95**, 9831-9838. https://doi.org/10.1021/acs.analchem.3c00691
13. X. Yan, Y. Song, C. Z. Zhu, H. X. Li, D. Du, X. G. Su, and Y. H. Lin, *Anal. Chem.*, 2018, **90**, 2618-2624. https://doi.org/10.1021/acs.analchem.7b04193
14. D. Q. Han and Z. P. Yao, *TRAC-Trend. Anal. Chem.*, 2020, **123**, 115763. https://doi.org/10.1016/j.trac.2019.115763
15. I. F. Pinto, D. R. Santos, C. R. F. Caneira, R. R. G. Soares, A. M. Azevedo, V. Chu, and J. P. Conde, *J. Micromech. Microeng.*, 2018, **28**, 9. https://doi.org/10.1088/1361-6439/aac66c
16. B. Rajangam, D. K. Daniel, and A. I. Krastanov, *Eng. Life Sci.*, 2018, **18**, 4-19. https://doi.org/10.1002/elsc.201700028
17. B. Bucur, F. D. Munteanu, J. L. Marty, and A. Vasilescu, *Biosensors-Basel*, 2018, **8**, 27. https://doi.org/10.3390/bios8020027
18. A. V. Alex and A. Mukherjee, *Microchem. J.*, 2021, **161**, 105779. https://doi.org/10.1016/j.microc.2020.105779
19. M. L. Satnami, J. Korram, R. Nagwanshi, S. K. Vaishanav, I. Karbhal, H. K. Dewangan, and K. K. Ghosh, *Sensor. Actuat. B-Chem.*, 2018, **267**, 155-164. https://doi.org/10.1016/j.snb.2018.03.181
20. C. S. Pundir, A. Malik, and Preety, *Biosens. Bioelectron.*, 2019, **140**, 111348. https://doi.org/10.1016/j.bios.2019.111348
21. S. L. C. Ferreira, J. P. dos Anjos, C. S. A. Felix, M. M. da Silva, E. Palacio, and V. Cerda, *TRAC-Trend. Anal. Chem.*, 2019, **110**, 335-343. https://doi.org/10.1016/j.trac.2018.11.017
22. O. Alp and G. Tosun, *Food Chem.*, 2019, **290**, 10-15. https://doi.org/10.1016/j.foodchem.2019.03.119
23. P. P. Chen; P. Wu; J. B. Chen; P. F. Yang; X. F. Zhang; C. B. Zheng, and X. D. Hou, *Anal. Chem.*, 2016, **88**, 2065-2071. https://doi.org/10.1021/acs.analchem.5b03307
24. Q. Kang; B. B. Chen; M. He, and B. Hu, *Anal. Chem.*, 2022, **94**, 12934-12941. https://doi.org/10.1021/acs.analchem.2c03234
25. N. N. Tang; Z. X. Li; L. M. Yang, and Q. Q. Wang, *Anal. Chem.*, 2016, **88**, 9890-9896. https://doi.org/10.1021/acs.analchem.6b02979
26. R. Hou, Y. Gu, Y. Zhao, X. Zhao, L. Yang, X. Yan, and Q. Wang, *Atom. Spectrosc.*, 2024, **45**, 74-82. https://doi.org/10.46770/as.2024.078
27. X. Chen, X. Zhao, S. Pu, R. Liu, and Y. Lv, *Atom. Spectrosc.*, 2023, **44**, 427-433. https://doi.org/10.46770/as.2023.285
28. Y. Cai, Y. L. Yu, and J. H. Wang, *Anal, Chem,*, 2018, **90**, 10607-10613. https://doi.org/10.1021/acs.analchem.8b02904
29. X. M. Jiang, Y. Chen, C. B. Zheng, and X. D. Hou, *Anal. Chem.*, 2014, **86**, 5220-5224. https://doi.org/10.1021/ac500637p
30. S. Liu, X. X. Xue, Y. L. Yu, and J. H. Wang, *Anal, Chem,*, 2021, **93**, 6262-6269. https://doi.org/10.1021/acs.analchem.1c00819
31. X. Wang, T. Ren, Y. Yang, Y. Lin, Y. Deng, and C. Zheng, *Atom. Spectrosc.*, 2024, **45**. https://doi.org/10.46770/as.2024.142
32. Z. Cai and Z. Wang, *Atom. Spectrosc.*, 2023, **44**, 354-364. https://doi.org/10.46770/as.2023.190
33. Y. R. Zhang, J. X. Liu, X. F. Mao, G. Y. Chen, and D. Tian, *TRAC-Trend. Anal. Chem.*, 2021, **144**. https://doi.org/10.1016/j.trac.2021.116437
34. H. Y. Yang, L. P. Qi, J. R. Zhou, Q. Li, X. Yuan, M. Zhang, Y. He, K. Huang, and P. P. Chen, *Anal. Chim. Acta.*, 2023, **1262**, 341223. https://doi.org/10.1016/j.aca.2023.341223
35. Y. P. Wang, Y. M. Chen, K. J. Li, J. R. Zhou, X. Yuan, M. Zhang, and K. Huang, *Anal. Chim. Acta.*, 2024, **1287**, 8, 342064. https://doi.org/10.1016/j.aca.2023.342064
36. J. J. Xiao, X. Xu, F. Wang, J. J. Ma, M. Liao, H. Shi, Q. K. Fang, and H. Q. Cao, *J. Hazard. Mater.*, 2019, **365**, 857-867. https://doi.org/10.1016/j.jhazmat.2018.11.075

37. J. Z. Ruan, G. T. Li, X. Y. Lu, D. L. Wang, Z. Yang, S. J. Wang, and X. M. Ji, *J. Food Compos. Anal.* 2023, **121**, 105403. https://doi.org/10.1016/j.jfca.2023.105403
38. V. Tripathy, A. Saha, and J. Kumar, *J. Food Sci. Tech. Mys.*, 2017, **54**, 458-468. https://doi.org/10.1007/s13197-017-2487-x
39. X. Y. Luo, X. Zeng, D. D. Wei, C. C. Ma, J. H. Li, X. H. Guo, L. H. Cheng, and Z. X. Mao, *Food Addit. Contam. B*, 2023, **16**, 244-252. https://doi.org/10.1080/19393210.2023.2214797
40. P. P. Chen, C. B. Zheng, C. Chen, K. Huang, X. Wang, P. Y. Hu, and J. Geng, *Anal. Chim. Acta*, 2020, **1111**, 8-15. https://doi.org/10.1016/j.aca.2020.03.031
41. K. Mwila, M. H. Burton, J. S. Van Dyk, and B. I. Pletschke, *Environ. Monit. Assess.*, 2013, **185**, 2315-2327. https://doi.org/10.1007/s10661-012-2711-0
42. J. S. Van Dyk, and B. Pletschke, *Chemosphere*, 2011, **82**, 291-307. https://doi.org/10.1016/j.chemosphere.2010.10.033